(12)

Corrosion Resistance of Metal Matrix Composites

FINAL REPORT
to

Office of Naval Research
Grant No. N00014-89-J-1588

by
Professor R. M. Latanision

The H. H. Uhlig Corrosion Laboratory
Department of Materials Science and Engineering
Massachusetts Institute of Technology
Cambridge, Massachusetts 02139

October 1992

3

SECURITY CLASSIFICATION OF THIS PAGE

REPORT DOCUMENTATION PAGE

Form Approved
OMB No 0704-0188

1a REPORT SECURITY CLASSIFICATION Unclassified	1b RESTRICTIVE MARKINGS
2a SECURITY CLASSIFICATION AUTHORITY	3 DISTRIBUTION / AVAILABILITY OF REPORT
2b DECLASSIFICATION / DOWNGRADING SCHEDULE	
4 PERFORMING ORGANIZATION REPORT NUMBER(S)	5 MONITORING ORGANIZATION REPORT NUMBER(S)
6a NAME OF PERFORMING ORGANIZATION Massachusetts Institute of Technology 6b OFFICE SYMBOL (If applicable)	7a NAME OF MONITORING ORGANIZATION Office of Naval Research
6c ADDRESS (City, State, and ZIP Code) Room 8-202, 77 Massachusetts Avenue Cambridge, MA 02139	7b ADDRESS (City, State, and ZIP Code) 800 N. Quincy Street Arlington, VA 22217-5000
8a NAME OF FUNDING / SPONSORING ORGANIZATION Office of Naval Research 8b OFFICE SYMBOL (If applicable)	9 PROCUREMENT INSTRUMENT IDENTIFICATION NUMBER
8c ADDRESS (City, State, and ZIP Code) Arlington, VA 22217-5000	10 SOURCE OF FUNDING NUMBERS PROGRAM ELEMENT NO: 89-J-1588 / PROJECT NO: cor5523-02 / TASK NO: / WORK UNIT ACCESSION NO:

11 TITLE (Include Security Classification)
Corrosion Resistance of Metal Matrix Composites

12 PERSONAL AUTHOR(S)
R. M. Latanision

13a TYPE OF REPORT	13b TIME COVERED	14 DATE OF REPORT (Year, Month, Day)	15 PAGE COUNT
Final Report	FROM Mar 89 TO Oct 92	October 1992	

16 SUPPLEMENTARY NOTATION

17 COSATI CODES			18 SUBJECT TERMS (Continue on reverse if necessary and identify by block number)
FIELD	GROUP	SUB-GROUP	Corrosion, Graphite Aluminum Metal Matrix Composites

19 ABSTRACT (Continue on reverse if necessary and identify by block number)

This program examined the relationship between processing and chemistry in continuous fiber graphite/aluminum alloy metal mix composites (G/Al MMCs) with particular attention to subsequent effects on electrochemical behavior. In general, anodic polarization of G/Al MMCs compared well with mixed electrode model predictions. Deviations were associated with commercial fiber type and interfacial intermetallics. At high anodic overpotentials, graphite fiber oxidation and subsequent crevice formation resulted in large deviations from mixed-potential theory. Zinc ion implantation of graphite fibers was found to reduce the corrosion rate by a factor of twenty in NaCl solutions. Al_4C_3 hydrolysis was not observed on the time scale of the polarization studies performed. The scanning potential microprobe (SPM) was used to identify cathodic and anodic sites *in situ* for both model G/Al composites and commercial 0-90° interlaminar G/6061 Al MMCs.

20 DISTRIBUTION / AVAILABILITY OF ABSTRACT ☒ UNCLASSIFIED/UNLIMITED ☐ SAME AS RPT ☐ DTIC USERS	21 ABSTRACT SECURITY CLASSIFICATION Unrestricted
22a NAME OF RESPONSIBLE INDIVIDUAL A. J. Sedriks	22b TELEPHONE (Include Area Code) (202) 696-4401 22c OFFICE SYMBOL 1131 M

DD Form 1473, JUN 86 *Previous editions are obsolete.* SECURITY CLASSIFICATION OF THIS PAGE

S/N 0102-LF-014-6603

1. INTRODUCTION

Currently, fibrous graphite aluminum (G/Al) metal matrix composites (MMCs) are being considered for structural components in aircraft and other applications where specific strength and weight savings are important parameters [Meyers, et al., 1984; Mortensen, 1988a; Taya, et al., 1989]. However, in part because they are susceptible to galvanic corrosion [Hack and Amateau, 1983; Aylor, et al., 1983; Czyrklis, 1985], their application has been limited. It has long been known that there is a synergistic corrosion effect due to the galvanic electrical contact at the fiber-matrix interface in G/Al MMCs. Therefore, G/Al MMC parts are usually fabricated with a protective coating (e.g., covering exposed areas with aluminum foil) to avoid such galvanic problems; however, it has been shown that such structures can be compromised during fabrication, structural assembly, usage, or by the chemical environment [Payer and Sullivan, 1976; Aylor, et al., 1983, 1984; Mansfield, et al., 1988, 1990].

Chemical passivation of Al-foil linings on G/Al MMCs and, more recently the composite itself, has been used to increase corrosion resistance [Mansfield, et al., 1988, 1990]. Although these techniques improve the corrosion resistance of MMCs, it is desirable to further improve the corrosion characteristics of the inherent composite fiber-matrix couple to ensure the integrity of the components in the event the surface foils should be compromised during service. It is also necessary that remedies to reduce corrosion (e.g. insulating coatings, matrix modification, revised processing conditions, etc.) do not degrade the mechanical properties of G/Al MMCs in such a way as to preclude their use.

The corrosion of G/Al MMCs has been studied extensively [Hihara, 1989; Dull, et al., 1977; Aylor, et al., 1984, 1985], and the galvanic effect in MMCs was modeled with the mixed-electrode theory [Hihara, 1989]. In the past, commercial G/Al MMCs studied were produced by a process known as diffusion-bonding. This process left behind trace microstructural chlorides, which increased the corrosion rate of the composite significantly [Hihara and Latanision, 1989, 1990, 1991]. Hihara [1989] determined that the anodic potentiodynamic behavior of diffusion-bonded commercial G/Al MMCs deviated significantly from that which was predicted by the mixed-electrode theory. The present study compares the anodic potentiodynamic behavior of several commercial G/Al MMCs, produced without microstructural chlorides in deaerated 0.5M Na_2SO_4 and 3.15 wt.% NaCl solutions.

Since the galvanic corrosion behavior of G/Al MMCs has been well established, it was decided that the problem of controlling corrosion should be addressed. In this study, Buonanno [1992] and Hihara[1989] considered cathodic protection, electrical insulation of fibers, and ion implantation of graphite with cathodic inhibitors as corrosion-control schemes for G/Al MMCs.

Previous work on G/Al MMCs suggested that the corrosion behavior of these composites may have been strongly related to the processing conditions employed during fabrication [Hihara, 1987, 1988b]. In order to derive the benefit of these advanced high specific strength materials, it is necessary to be able to control the parameters which govern the chemical stability of a material. It is well known that the formation of aluminum carbide (Al_4C_3) takes place when molten Al is in contact with graphite fibers [Amateau, 1976]. Subsequently, in the presence of an aqueous solution, hydrolysis of Al_4C_3 with methane evolution occurs. This reaction degrades the mechanical strength and structural integrity of G/Al MMCs by destroying the interface where Al_4C_3 forms. Therefore, the present work attempts to determine the relationship between Al_4C_3 content and the chemical stability of G/Al MMCs. In order to accomplish this, composites were produced with careful control and monitoring of processing conditions and examined by DC potentiodynamic polarization.

2. FINDINGS

2.1 Anodic Polarization of G/Al MMCs

One of the major goals of the present study was to consider the effect of Al_4C_3 at the fiber-matrix interface on the anodic polarization behavior of the G/Al MMCs during DC potentiodynamic polarization. The following section discusses the effect of Al_4C_3 hydrolysis on the anodic polarization behavior of the G/Al MMCs with Al_4C_3 contents measured by gas chromatography.

2.1.1 Al_4C_3 at the Fiber-Matrix Interface

The difference in Al_4C_3 content for G/1100 Al MMCs Specimen 1 (92 mg/m^2) and Specimen 2 should not have been significant, since they were processed with the same cooling rate (Figure 1). However, the difference in the passive current densities after anodic polarization was significant. Furthermore, G/Al 1100 MMCs with differing Al_4C_3 contents (Specimens 3 and 4: 69 mg/m^2 and 40 mg/m^2, respectively) did not show a significant difference in anodic passive current densities. Similar results were found for G/6061 Al MMCs.

Therefore, the Al_4C_3 content of a particular G/Al MMC did not correlate with the magnitude of the passive current densities measured by DC potentiodynamic polarization at the scan rate used (0.167 mV/s). If a slower scan rate had been used, it is possible that hydrolysis of Al_4C_3 would have shown a more pronounced effect on the anodic polarization behavior. However, the scan rate employed is accepted as a near equilibrium scan rate [Annual Book of ASTM Standards, 1991b].

2.1.2 Predicted Anodic Polarization Behavior from Mixed-Electrode Theory

The predicted anodic behavior of a 65% pitch-based G/Al MMC and the average anodic polarization behavior measured for the commercial G/Al MMCs tested are shown in Figure 2. Also shown in the figure is the anodic polarization behavior of a G/1100 Al MMC which had the lowest passive current density (Specimen 2). The curve of the latter specimen attained nearly the same shape and magnitude as that predicted by the mixed-electrode theory. As can be seen in Figure 2, the diffusion-bonded G/6061 T6-Al MMC studied by Hihara [1989] deviated significantly from mixed-electrode theory. Hihara determined that this was a result of microstructural chlorides in the matrix. The G/6061 Al MMC processed in the absence of microstructural chlorides showed considerably closer resemblance to the predicted anodic behavior, although the deviation in the passive current density is still considerable. This deviation was attributable to crevice corrosion observed at the fiber-matrix interface.

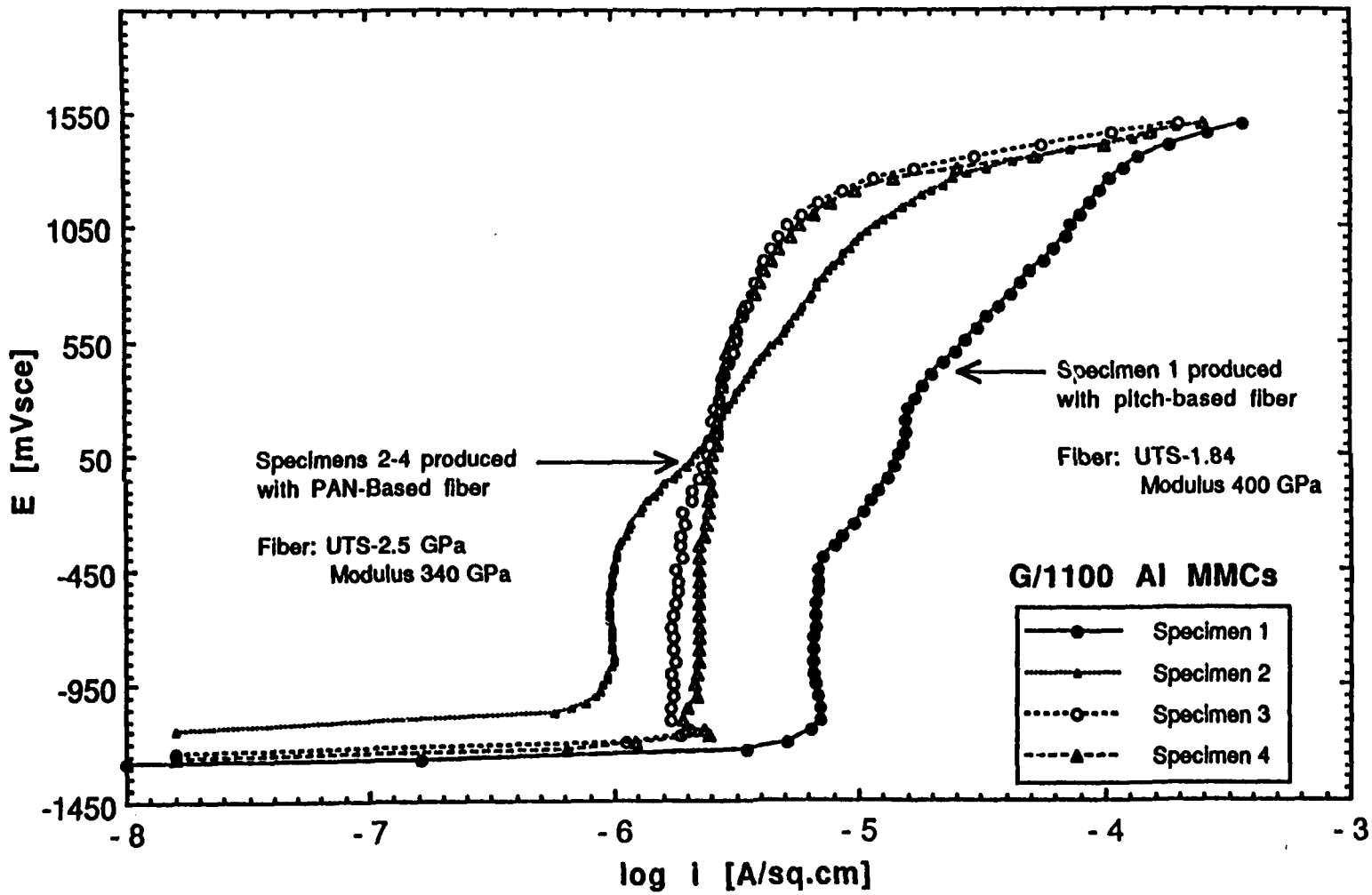

Figure 1: Comparison of anodic polarization results from G/1100 Al MMCs in deaerated 0.5M Na_2SO_4 solution of pH 7 at 30°C. Scan rate = 0.167 mV/s.

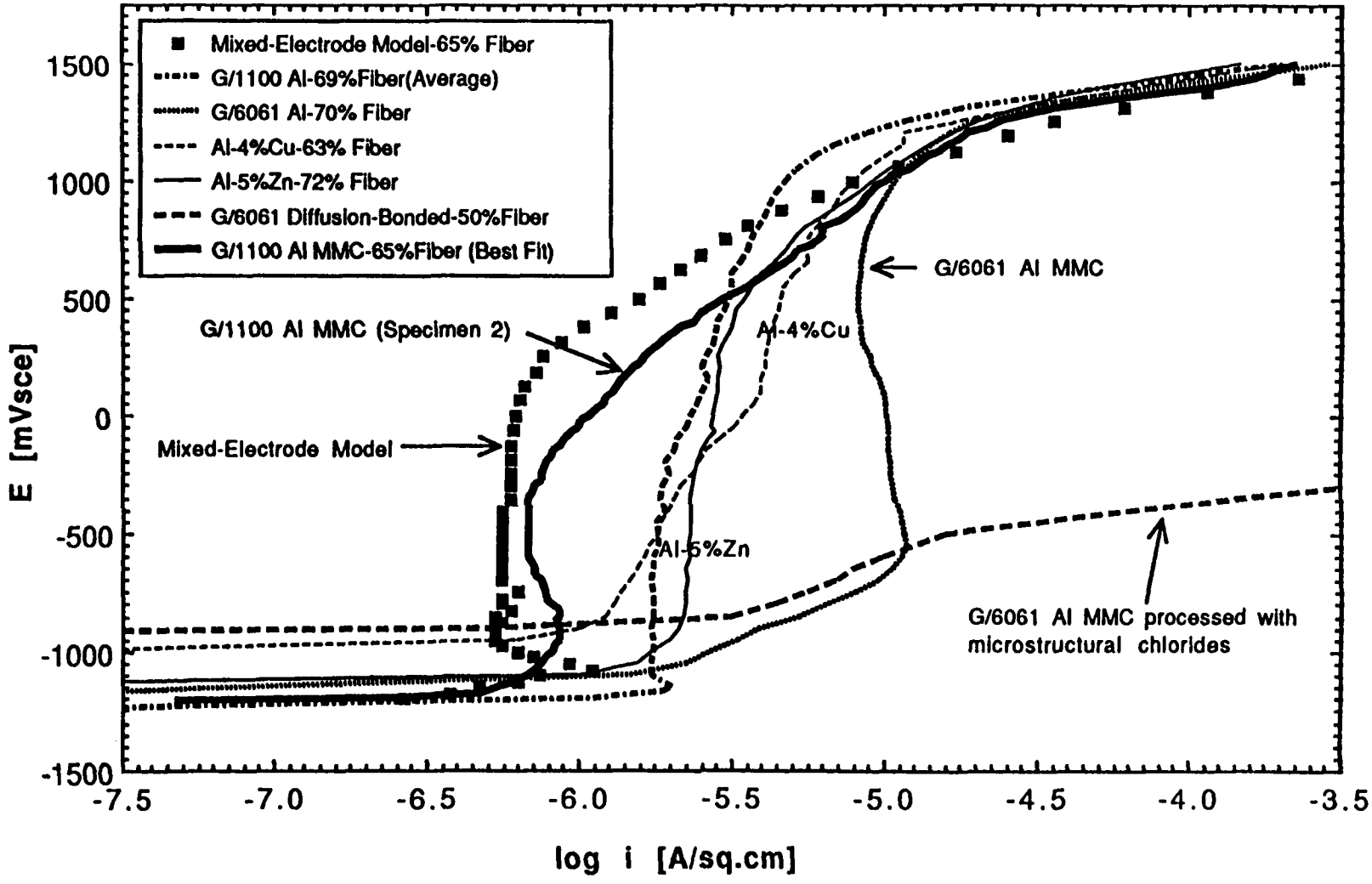

Figure 2: Predicted anodic polarization as a function of fiber vol.% graphite fiber reinforcement plotted against best experimental polarization results from G/Al MMCs with 1100 Al, 6061 Al, Al-4 wt.% Cu, Al-5 wt.% Zn, and 6061-T6 Al (with chlorides present) matrices in deaerated 0.5M Na_2SO_4 of pH 7 at 30°C. Scan rate = 0.167 mV/s.

The average anodic polarization behavior for the G/Al MMCs fabricated with the same PAN-based fiber shown in Figure 2 and with 4% Cu, 5% Zn, and no alloying elements (G/1100 Al MMCs) in the Al matrix was nearly the same. The tests show that alloy additions and Al_4C_3 content were not as significant in affecting the passive current density as was the type of graphite fiber used in processing the composites. To illustrate this more clearly, Figure 3 was constructed.

In Figure 3, the aforementioned composites that exhibited anomalous anodic polarization behavior are plotted. Although these two specimens had different matrix alloys, their general anodic polarization behavior was nearly the same. The addition of noble Cu to the matrix acts to raise the electrochemical potential of the composite; therefore, the specimen with the Cu alloy addition is shifted ~100 mVsce in the noble (positive) direction.

After noting that both specimens had PAN-based Torayca M40 3k fibers, a comparison between the pitch-based G/1100 Al MMC (Specimen 1) and the G/6061 Al MMCs which were fabricated with the same graphite fiber (Thornel P55s) was made; the magnitudes of the anodic passive current densities were also very similar.

Anodic oxidation of fibers or fiber dissolution, as it has already been pointed out, will occur during anodic polarization, with the principal product being CO_2 gas. Like graphite anodes used for Al reduction in the Hall process [Elliott and Tien, 1981], graphite will have an oxidation efficiency which is dependent on the chemistry and prior process treatment of the graphite. In general, the higher the fiber modulus, the greater the anodic current density will be for the composites at higher anodic overpotentials, as was shown for G/Al-Cu MMCs. Composites fabricated with high modulus Thornel 55s pitch-based fibers (modulus 44 GPa) had higher passive current densities during anodic polarization than composites fabricated with high modulus Courtaulds PAN-based fibers (modulus 340 GPa), which are reported to have a greater interfacial reactivity toward Al_4C_3 formation than pitch-based graphite fibers.

The more difficult issue is to determine how different fiber types affect the anodic corrosion density measurements. It is only possible to speculate upon which factors may have come into play. In Figure 4, an increase in the anodic current density occurred at approximately -200 mVsce for almost all G/Al-Cu MMCs. At this potential, the additional current results from the anodic oxidation of the graphite fibers. At potentials noble (positive) to -200 mVsce the difference in anodic polarization current density measurements are associated with the commencement of oxidation of graphite fiber; however, at potentials active (negative) to -200 mVsce, the measured current densities for the G/Al MMCs were often one or two decades greater than that predicted by mixed-electrode theory. This latter result requires further analysis.

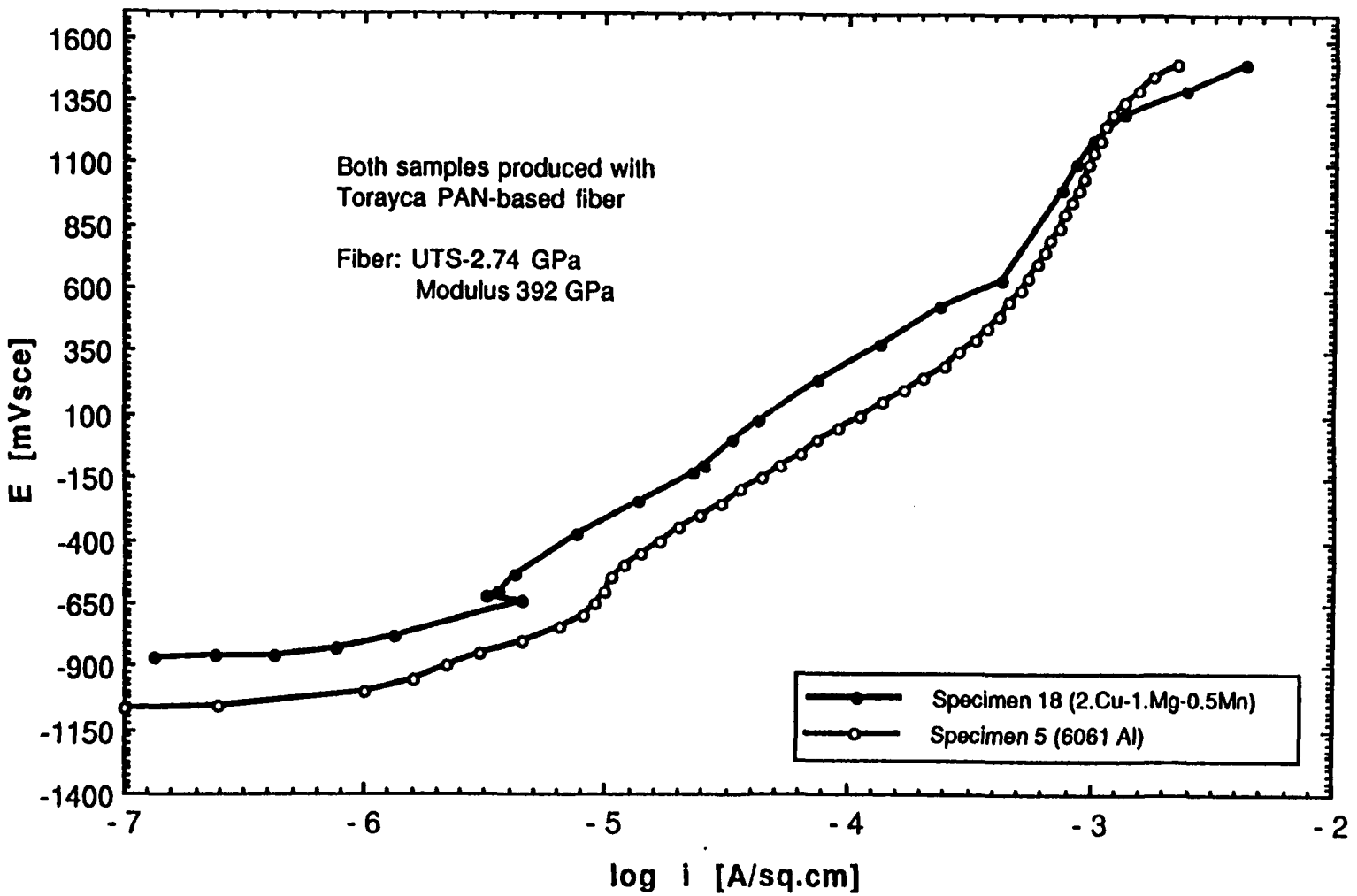

Figure 3: Comparison of anodic polarization results from G/Al-2% Cu MMC with Mg and Mn additions and a G/6061 Al MMC fabricated with the same graphite fiber in deaerated 0.5M Na_2SO_4 of pH 7 at 30°C. Scan rate = 0.167 mV/s.

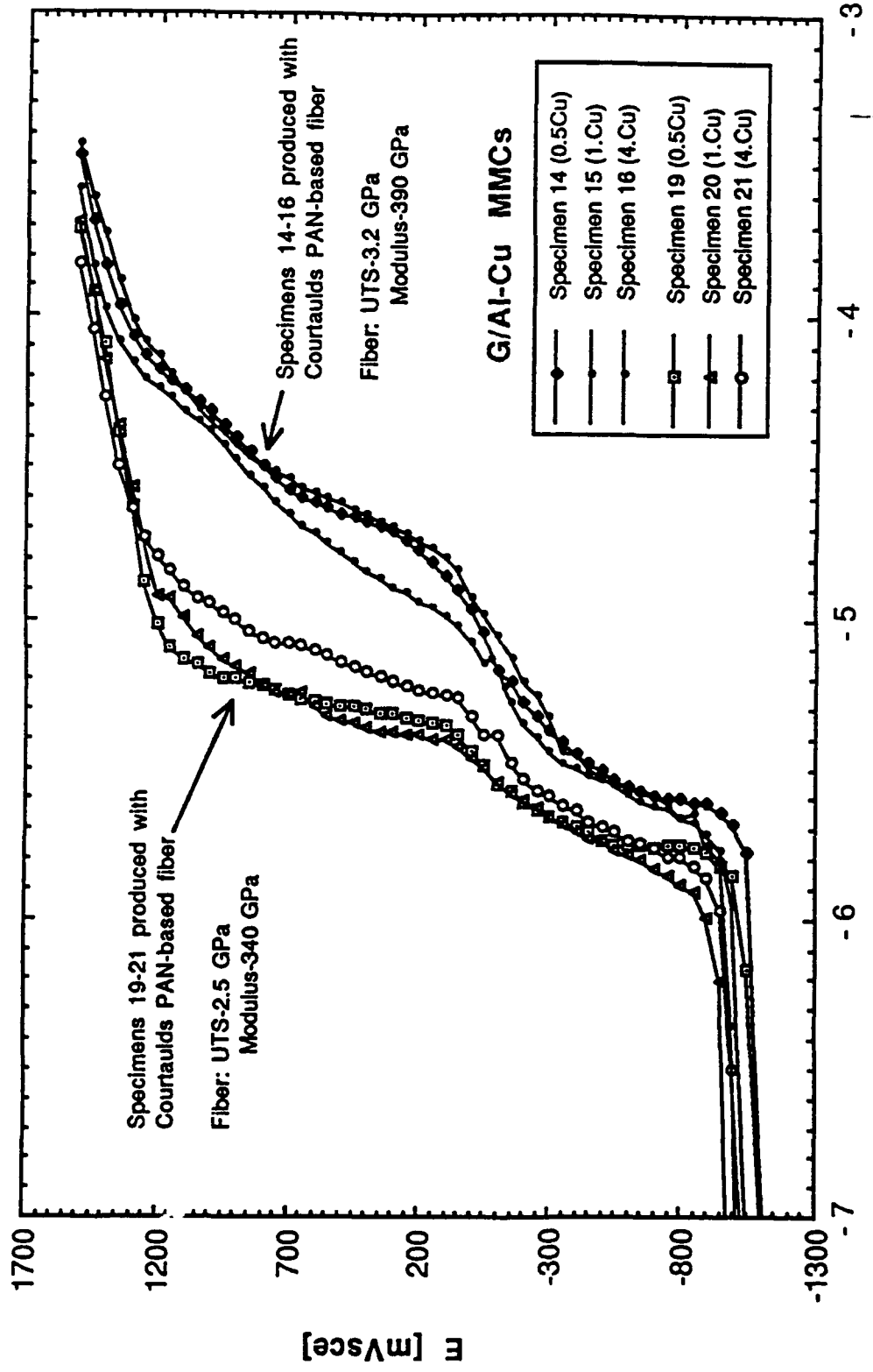

Figure 4: Comparison of anodic polarization results from G/Al-Cu MMCs with two different graphite fiber types in deaerated 0.5M Na_2SO_4 solution of pH 7 at 30°C. Scan rate = 0.167 mV/s.

The pre-existence or formation of crevices at potentials active to -200 mVsce will increase measured anodic current densities. Pitch-based G/6061 Al MMCs formed crevices readily during anodic polarization in deaerated 0.5M Na_2SO_4 solution, while G/Al MMCs with Courtaulds PAN-based fibers did not form crevices in 0.5M Na_2SO_4 solution. For the G/6061 Al MMCs, the deviation in anodic polarization behavior from that predicted by mixed-electrode theory was attributable to the distribution and morphology of the interfacial carbide and associated interfacial segregant which resulted in subsequent crevice corrosion. For the G/1100 (99.99 wt.%) al MMCs studied, the deviation from mixed-electrode theory (see Figure 2) at potentials below the equilibrium potential for CO_2 (34 mVsce) or CO (-277 mVsce) gas evolution has not been determined. The increase in measured passive current density may also be due to sub-micron crevice corrosion which was not observable under optical light microscopy.

Exposure to aerated NaCl solution and the etchant which was used for metallography resulted in cavern formation on the surface of the Courtaulds PAN-based graphite fiber. The degradation of the graphite fibers suggests that in the presence of an Al matrix, graphite fiber is not inert. The susceptibility of individual commercial fibers to cavern formation warrants further investigation. Chemical impurities in graphite may also be related to the observed phenomenon.

For the G/1100 (99.99 wt.%) Al MMCs studied, the anodic behavior of commercial G/Al MMCs compares well with that predicted by the mixed-electrode model (see Figure 2: Specimen 2). However, if a particular fiber reacts in such a way as to be later prone to crevice corrosion via carbide and segregation interplay at the interface (e.g., pitch-based G/6061 Al MMCs), then the mixed-electrode model is too conservative an estimate, since it assumes that no other phenomenon besides galvanic corrosion will take place when two materials are coupled.

The results show that Courtaulds PAN-based fibers are preferable to all other graphite fibers tested. Results from anodic polarization testing of specimens which were produced with these fibers were in fair agreement with that predicted by the mixed-electrode model. One G/Al 1100 MMC (Specimen 2) showed nearly the same anodic polarization behavior as that predicted by the mixed-electrode model (see Figure 2).

2.2 Anodic Polarization in Deaerated NaCl Solution

Ecrit for G/1100 (99.99 wt.%) Al MMCs was similar to that determined for high purity (99.999 wt.%) Al under similar conditions (see Table 1); therefore, Ecrit for the Al in the composite was not affected by the presence of graphite fibers.

Table 1: Corrosion Parameters Determined for G/Al MMCs in Deaerated 3.15 wt.% NaCl Solution

Specimen Number	Specimen Matrix	Ecorr mVsce	Ecrit mVsce	Eprot mVsce	i_p $\mu A/cm^2$
	pure Al (99.999%)	-1400	-750	N/A	0.63
	6061-T6 Al	-1220	-725	N/A	1
G Fiber	Composite 1100 Al				
2	"	-1155	-760	-950	1.8
3	"	-1240	-780	-960	5
4	"	-1140	-757	-1000	1.8
	6061 Al				
6	"	-1055	~-850	none	none
7	"	-1100	~-850	none	none
8	"	-1090	~-850	-978	10
9	"	-1080	~-850	N/A	1.8
	Al-Cu				
14	0.5% Cu	-1020	-700	N/A	6.3
15	1.% Cu	-1020	-710	N/A	10
16	4.% Cu	-1010	-790	N/A	6.3
17	2.% Cu	-990	-700	N/A	5.6
	0.7% Mg				
	0.3% Mn				
	Al-Cu				
19	0.5% Cu	-1037	-700	-920	5.6
20	1.% Cu	-1060	-710	-840	3.2
21	4.% Cu	-1030	-825	none	3
22	2.% Cu	-1025	-700	N/A	1.9
	0.7% Mg				
	0.3% Mn				
	Al-Zn				
10	0.1% Zn	-1060	-780	N/A	3.2
11	0.5% Zn	-1000	-770	-940	3.2
12	1.% Zn	-975	-975	none	none
13	5.% Zn	-980	-980	none	none

N/A = not available

On the other hand, no true Ecrit for the G/6061 Al MMCs was found during anodic polarization (see Figure 5). It has been observed that crevices formed in G/6061 Al MMCs at the fiber-matrix interfaces. However, no correlation could be found between Al_4C_3 content of the G/6061 Al MMCs and the values obtained for Ecrit values and passive current densities in deaerated 3.15 wt.% NaCl solution. The corrosion current densities measured were not directly proportional to the amount of observable crevice formation, since crevice corrosion is a localized phenomenon. Bruun and Nielsen [1991] have found similar corrosion behavior for continuous alumina fiber/6061 Al MMCs. They claim that Al_8Mg_5 and Mg_2Si provided "tunnel-like" corrosion paths along the fiber-matrix interface. Dull, et al. [1977] found high passive current densities on G/6061 Al MMCs but did not report the formation of crevices at the fiber-matrix interface. Their G/6061 Al MMCs had an Ecrit of -753 mVsce, nearly the same value of Ecrit found by Hihara [1989] for monolithic 6061 T6-Al. Their squeeze cast G/6061 Al MMCs composites were fabricated with pitch-based (Thornel 50) fibers. This suggests that the results obtained for the G/6061 Al MMCs used in this study may have been related to increased interfacial reaction and segregation resulting from the higher temperatures used during pressure infiltration as opposed to squeeze casting.

Limited concentrations of Cu (0.5 wt.%) or Mg (0.7 wt.%) added to the Al matrix seem to have a beneficial effect on the pitting resistance in G/Al-Cu MMCs in deaerated NaCl solution. The reason for this is not yet clear. It may be due to fine-scale pitting occurring at sub-micron $CuAl_2$ (θ) eutectic precipitates in fiber interstices. This fine-scale pitting phenomenon has been observed by Trzaskoma [1991] in particulate reinforced SiC/Al MMCs; the refinement of precipitates in the Al matrix resulted in a more noble Ecrit, presumably by increasing the number of pits which form, and hence, pit growth competition.

2.3 Surface Analysis of G/Al MMCs Exposed to Aerated NaCl Solution

XPS analysis integrated with SEM micrographs, revealed that the G/Al-5% Zn MMC was oxidized to a greater extent than the G/1100 Al MMC. A thicker more discontinuous corrosion product had formed on the surface of the G/Al-5% Zn MMC, while the matrix had also pitted to a greater extent due to the addition of Zn in the matrix. XPS analysis confirmed the presence of $Zn(OH)_2$ on the surface of the G/Al-5% Zn MMC. Because of the poor spatial resolution of XPS analysis, the location of $Zn(OH)_2$ can only be said to have occurred where no voluminous $Al(OH)_3$ corrosion product was observed.

SEM and AES mapping confirmed that small thin gray areas of a discontinuous Al-Zn oxide film were present on the surfaces of fibers, while Zn was found by AES elemental mapping to have segregated to the fiber-matrix interface. Evidently, the gray Al-Zn oxide film did not suppress oxygen reduction on the time scale of the test (24 hours), since corrosion proceeded at a greater extent in the G/Al-5% Zn MMC as compared to the G/1100 Al MMC.

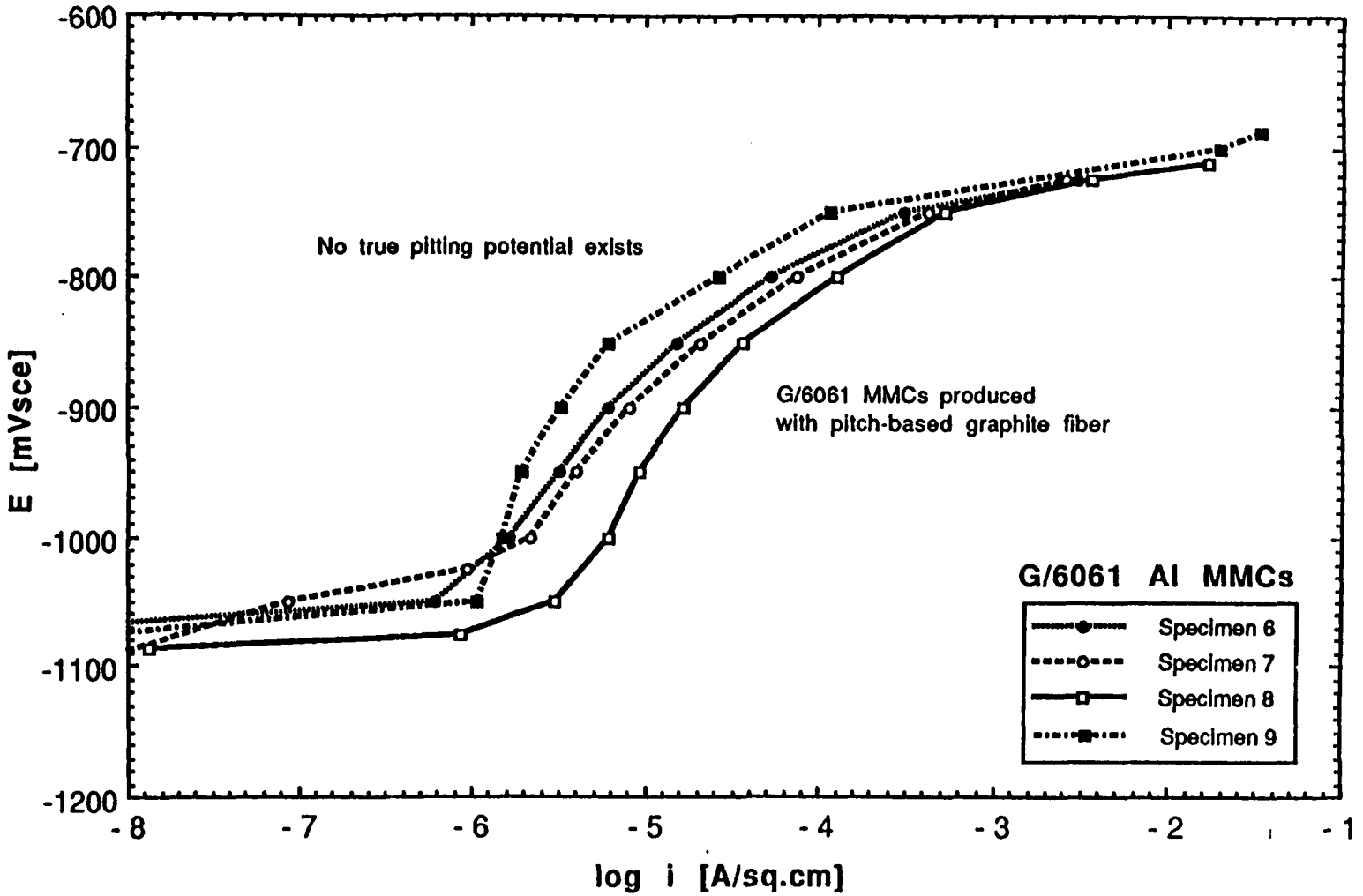

Figure 5: Comparison of anodic polarization results from G/6061 Al MMCs in deaerated 3.15 wt.% NaCl solution of pH 7 at 30°C. Scan rate = 0.167 mV/s.

Pitting corrosion in Al channels was observed for the G/Al-Zn MMCs exposed to aerated 3.15 wt.% NaCl solution. Therefore, Al channels in G/Al MMCs should be avoided from an electrochemical perspective.

2.4 SPM Analysis of Model G/Al MMCs

Of the two Zn ion-implanted specimens tested, only the specimen with an 11mm diameter showed a consistent decrease in corrosion current densities after 48 hours (see Figures 6 through 8). Both the cathodic and anodic current densities decreased significantly after a period of 24 hours. For the 11mm diameter Zn ion-implanted specimen, the cathodic current density decreased by a factor of 12 after 24 hours; while after 48 hours, the cathodic current density had dropped by a factor of 20 from the initial cathodic current density. The 16mm diameter Zn ion-implanted specimen showed a similar decrease in corrosion current densities after 24 hours; however, after 48 hours, both the anodic and cathodic current density values began to increase as a large crevice formed at the G/Al interface. One possible explanation for the different behavior is that the anodic area was greater for the 16mm diameter Zn ion-implanted specimen and, hence, the cathodic current density over the graphite rod was greater. Localized crevice corrosion had begun at the G/Al interface after only 24 hours in solution.

Zn ion-implanted specimens were examined by secondary ion mass spectroscopy (SIMS) after removal from solution; however, the presence of $Zn(OH)_2$ was not confirmed, since the concentration of ion-implanted Zn was at the threshold of the detection limit of the instrument. It is probable that in solution Zn cations subsequently formed $Zn(OH)_2$ film over graphite, and thus, the cathodic oxygen reduction reaction decreased as observed. Therefore, ion implantation of Zn in graphite may be a viable means to reduce the driving force for galvanic corrosion in G/Al MMCs and warrants further investigation.

2.5 SPM Analysis of Commercial G/Al MMCs

The results of SPM analysis of 0-90° interlaminar G/6061 Al MMCs reveal that macroscopic galvanic cells formed between the interlaminar layers (see Figures 9 and 10). The formation of the galvanic cells is most likely influenced by the difference in the surface energy of the exposed graphite fibers, since the internal C-C bond energy of the transverse fibers will be markedly different from the surface energy of the longitudinally exposed fibers; therefore, the rate of oxygen reduction should be different on the graphite fibers in alternate interlaminar regions. However, several SPM analyses showed that the net ionic current density determined above exposed transverse graphite fiber interlaminar regions as compared to exposed longitudinal graphite fiber regions was not always the same. This suggests that system is complicated by the local vol.% fiber and amount of Al matrix (i.e., the net ionic current density is a resultant of the distribution of current sources on the specimen surface).

Figure 6: Video image of an Zn-implanted G/Al MMC specimen with an 11mm outer Al diameter at time = 0. SPM current density vectors have been superimposed. Solution 0.01 M NaCl open to air. pH~7

Figure 7: Video image of an Zn-implanted G/Al MMC specimen with an 11mm outer Al diameter at time = 24 hrs. SPM current density vectors have been superimposed. Solution 0.01 M NaCl open to air. pH~7

Figure 8: Video image of an Zn-implanted G/Al MMC specimen with an 11mm outer Al diameter at time = 48 hrs. SPM current density vectors have been superimposed. Solution 0.01 M NaCl open to air. pH~7

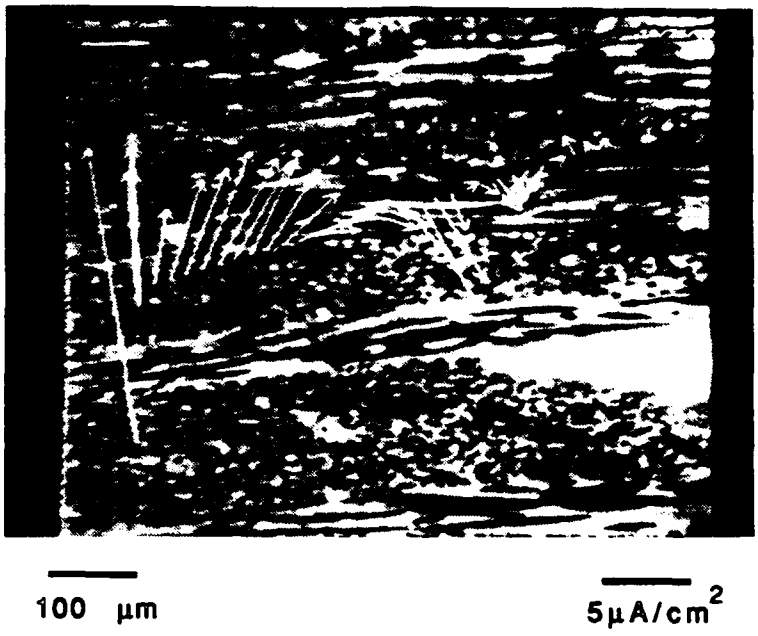

Figure 9: SPM video image of a G/6061 Al MMC (Specimen 25) with 0-90° fiber plies; current density vectors are superimposed. Solution 0.01 M NaCl open to air. pH~7

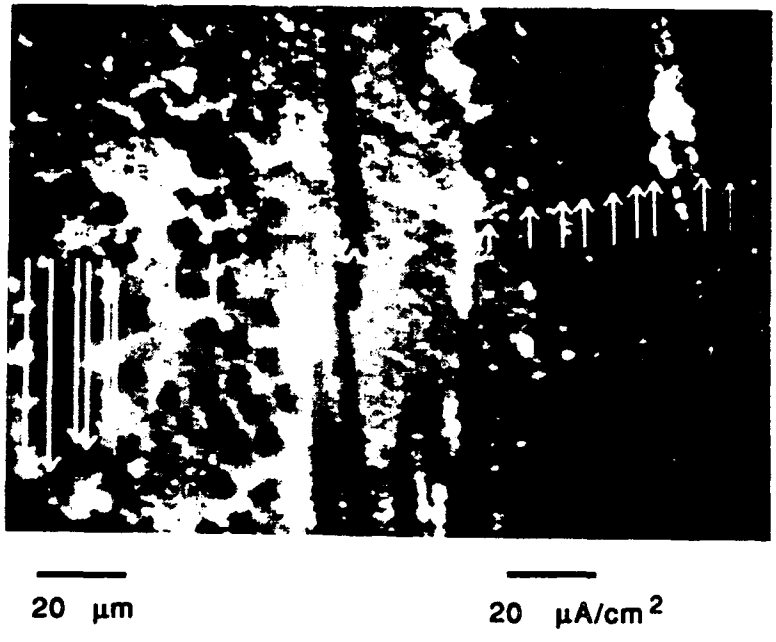

Figure 10: SPM video image of a G/6061 Al MMC (Specimen 25) with 0-90° fiber plies; current density vectors are superimposed. Solution 0.01 M NaCl open to air. pH~7

During the ongoing process of corrosion, greater fiber surface areas will be achieved as a result of matrix corrosion, and as time progresses, the corrosion rates of composites in contact with an electrolyte will not remain constant. Fluctuating cathodic and anodic sites may act to increase corrosion.

Finally, the SPM was a valuable tool for studying the corrosion behavior of MMCs, as it was able to conclusively identify cathodic and anodic sites in large scale model G/Al MMCs. It also led to the verification of macroscopic corrosion phenomena in commercial MMCs which had fiber diameters at the resolution of the probe tip. The increased corrosion for 0-90° interlaminar G/6061 Al MMCs was explained by 'macroscopic' electrochemical cells which were created by local differences in graphite fiber: a result of fiber distribution and orientation.

3. CONCLUSIONS OF THIS PROGRAM

From the experimental results obtained in this present work the following conclusions can be drawn:

3.1 DC ELECTROCHEMICAL STUDIES

1. The commercial fiber type strongly affected the polarization behavior of the G/Al MMCs studied. Anodic oxidation of high modulus and high strength fibers resulted in increased passive current densities and crevice formation at the G/Al interface.

2. Anodic polarization of G/Al MMCs approached that predicted by the mixed-electrode theory. However, the passive current densities attained for G/6061 Al MMCs were well above those predicted by the theory due to crevice corrosion at the G/Al interface. No true pitting potential was found for G/6061 Al MMCs due to crevice corrosion.

3. G/Al-0.5% Cu MMC and G/Al-2% Cu MMC with 0.7% Mg and 0.3% Mn additions showed better pitting resistance than similar fiber type G/1100 Al MMCs and monolithic Al in deaerated 3.15 wt.% NaCl solution.

4. Zn additions above 1 wt.% in G/Al MMCs strongly decreased the pitting resistance of the composite in deaerated 3.15 wt.% NaCl solution.

5. As expected, oxygen reduction on G/Al MMCs was easily attainable even for pure Al matrices due to the presence of graphite fibers; therefore, there was no advantage in using a pure Al matrix to deter corrosion in oxygenated conditions.

3.2 SPM STUDIES

1. The cathodic inhibition of oxygen reduction on graphite due to the presence of ion-implanted Zn was confirmed by SPM *in-situ* analysis. For samples with smaller anode to cathode ratios, the protection was complete after a period of 48 hours.

2. Corrosion due to macroscopic metallographic features was correlated with the interlaminar 0-90° construction of the composite and resulted in an order of magnitude increase in current density measurements as compared to that of continuous fiber similar G/Al MMCs.

4. REFERENCES

Amateau, M. F., "Progress in the Development of Graphite Aluminum Composite Using Liquid Infiltration Technology," Journal of Composite Materials, 10, 1976, p. 1281-1289.

Aylor, D. M. and Kain, R. M., "Assessing the Corrosion Resistance of Metal Matrix Composite Materials in Marine Environments," Recent Advances in Composites in the United States and Japan, Ed. by J. R. Vinson and M. Taya, ASTM Special Technical Publication, 864, 1983, p. 632.

Aylor, D. M. and Moran, P. J., "Effect of Reinforcement on the Pitting Behavior of Aluminum-Base Metal Matrix Composites," Journal of the Electrochemical Society, 132 (6), 1985, p. 1277.

Aylor, D. M.; Ferrara, R. J.; Kain, R. M., "Marine Corrosion and Protection for Graphite/Aluminum Metal Matrix Composites," Materials Performance, 23, (7), 1984, p. 32-38.

Bruun, N. K. and Nielsen, K., "Corrosion Resistance of Fibre Reinforced Aluminum," Metal Matrix Composites - Processing, Microstructure and Properties, Ed. by Hansen , et al., 12th Risø International Symposium on Materials Science, 1991, p.257-264.

Buonanno, M. A., "The Effect of Processing Conditions and Chemistry on the Electrochemistry of Graphite and Aluminum Metal Matrix Composites," Ph. D., MIT, 1992.

Czyrklis, W. F., "Corrosion Evaluation of Graphite-Aluminum and Graphite-Magnesium Metal Matrix Composites," Corrosion, 85, NACE, Paper No. 196, 1985.

Dull, D. L.; Harrigan, W. C., Jr.; Amateau, M. F., "Final Report: The Effect of Matrix and Fiber Composition on Mechanical Strength and Corrosion Behavior of Graphite-Aluminum Composites," The Aerospace Corporation, El Segundo, CA, Aerospace Report No. ATR-76 (7564)-1, 1977.

Elliot, J. F. and Tien, J. K., Metallurgical Treatises, USA-China Bilateral Conference (1981: Peking, China) Metallurgical Society of AIME, PA, p. 137-157.

Hack, J. E. and Amateau, M. F., eds., Mechanical Behavior of MMCs, Warrendale, PA: Metallurgical Society of AIME, 1983, p.335-352.

Hihara, L. H., Corrosion of Aluminum Matrix Composites, Ph.D. Thesis, MIT, Cambridge, MA, 1989.

Hihara, L. H. and Latanision, R. M., "Cathodic Overprotection of Silicon Carbide/6061-T6 and Graphite/6061-T6 Aluminum Alloy Metal Matrix Composites," Scripta Metallurgica, 22, 1988a, p. 413-418.

Hihara, L. H. and Latanision, R. M., "Localized Corrosion of Graphite Fiber/6061-T6 Aluminum Alloy Metal Matrix Composites in Aerated and Deaerated Sodium Sulfate Solutions," Space Age Metals Technology, Ed. by F. H. Froes and R. A. Cull, Covina, CA: SAMPE, 2, 1988b, p. 213.

Hihara, L. H. and Latanision, R. M., "Residual Microstructural Chloride in Graphite-Aluminum Metal Matrix Composites," Materials Science and Engineering, A126, 1990, p. 231-234.

Hihara, L. H. and Latanision, R. M., "Localized Corrosion Induced in Graphite/Aluminum Metal-Matrix Composites by Residual Microstructural Chloride," Corrosion, 47, (5), 1991, p. 335-341.

Mansfeld, F.; Lin, S.; Kim, S.; Shih, H., "Corrosion Protection of Al Alloys and Al-based Metal Matrix Composites by Chemical Passivation," Corrosion, 1988, Paper No. 388, p. 1-19.

Mansfeld, F.; Lin, S.; Kim, S.; Shih, H., "Pitting and Passivation of Al Alloys and Al-based Metal Matrix Composites," Journal of the Electrochem. Soc., 137, (1), 1990, p. 78-82.

Meyers, M. A. and Chawla, K. K., Mechanical Metallurgy Principles and Applications, Englewood Cliffs, NJ: Prentice-Hall, Inc., 1984, p. 438-466.

Mortensen, A.; Cornie, J. A.; Flemings, M. C., "Solidification Processing of Metal-Matrix Composites," Journal of Metals, (F) 1988a, p. 12-19.

Payer, J. H. and Sullivan, P. G., "Corrosion Protection Methods for Graphite Fiber Reinforced Aluminum Alloys," Bicentennial of Materials, 8th National Sample Technical Conference, Vol. 8, Society for the Advancement of Material and Process Engineering, Seattle, WA, October 12-14, 1976.

Taya, M. and Arsenault, R. J., Metal Matrix Composites' Thermomechanical Behavior, Elmsford, NY: Pergamon Press, 1989, p. 5-8.

Trzaskoma, P. P., "Localized Corrosion of Metal Matrix Composites, " Environmental Effects on Advanced Materials, Ed. by R. H. Jones and R. E. Ricker, The Minerals, Metals and Materials Society, 1991, p. 249-265.

BASIC DISTRIBUTION LIST

Technical Reports and Publications [illegible] Feb 1990

Organization	Copies
Defense Documentation Center Cameron Station Alexandria, VA 22314	12
Office of Naval Research Dept. of the Navy 800 N. Quincy Street Arlington, VA 22217 ATTN: Code 1131	3
Naval Research Laboratory Washington, DC 20375 ATTN: Codes 6000	1
6300	1
2627	1
Naval Air Development Center Code 606 Warminster, PA 18974 ATTN: Dr. J. DeLuccia	1
Commanding Officer Naval Surface Warfare Center Silver Spring, MD 20903-5000 ATTN: Library	1
Code R33	1
Naval Ocean Systems Center San Diego, CA 92152-5000 ATTN: Library	1
Naval Postgraduate School Monterey, CA 93940 ATTN: Mechanical Engineering Department	1
Naval Air Systems Command Washington, DC 20360 ATTN: Code 310A	1
Code 5304B	1
Code 931A	1
Naval Sea Systems Command Washington, DC 20362 ATTN: Code 05M	1
Code 05R	1

Organization	Copies
Naval Air Propulsion Center Trenton, NJ 08628 ATTN: Library	1
Naval Civil Engineering Laboratory Port Hueneme, CA 94043 ATTN: Materials Div.	1
Naval Electronics Laboratory San Diego, CA 92152 ATTN: Electronic Materials Sciences Division	1
Commander David Taylor Research Center Bethesda, MD 20084	1
Naval Underwater System Ctr. Newport, RI 02840 ATTN: Library	1
Naval Weapons Center China Lake, CA 93555 ATTN: Library	1
NASA Lewis Research Center 21000 Brookpark Road Cleveland, OH 44135 ATTN: Library	1
National Institute of Standards and Technology Gaithersburg, MD 20899 ATTN: Metallurgy Division	1
Ceramics Division	1
Fracture & Deformation Division	1

Naval Facilities Engineering
Command
Alexandria, VA 22331
ATTN: Code 03 1

Commandant of the Marine Corps 1
Scientific Advisor
Washington, DC 20380
ATTN: Code AX 1

Army Research Office
P.O. Box 12211
Research Triangle Park, NC 27709
ATTN: Metallurgy & Ceramics
Program 1

Army Materials Technology Laboratory
Watertown, MA 02172-0001
ATTN: Research Program Office 1

Air Force Office of Scientific
Research
Building 410
Bolling Air Force Base
Washington, DC 20332
ATTN: Electronics & Materials
Science Directorate 1

NASA Headquarters
Washington, DC 20546
ATTN: Code RM 1

Defense Metals & Ceramics
Information Center
Battelle Memorial Inst.
505 King Avenue
Columbus, OH 43201 1

Oak Ridge National Laboratory
Metals and Ceramics Div.
P.O. Box X
Oak Ridge, TN 37380 1
Oak Ridge, TN 37380 1

Los Alamos Scientific Lab.
P.O. Box 1663
Los Alamos, NM 87544
ATTN: Report Librarian 1

Argonne National Laboratory
Metallurgy Division
P.O. Box 229
Lemont, IL 60439 1

Brookhaven National Laboratory
Technical Information Division
Upton, Long Island
New York 11973
ATTN: Research Library 1

Lawrence Berkeley Lab.
1 Cyclotron Rd
Berkeley, CA 94720
ATTN: Library 1

David Taylor Research Ctr
Annapolis, MD 21402-5067
ATTN: Code 281 1
Code 2813 1
Code 0115 1

4315DIST
April 1991

Supplemental Distribution List

Profs. G.H. Meier and F.S.Pettit
Dept. of Metallurgical and
Materials Eng.
University of Pittsburgh
Pittsburgh, PA 15261

Prof. H.K. Birnbaum
Dept. of Metallurgy
& Mining Eng.
University of Illinois
Urbana, Il 61801

Prof. H.W. Pickering
Dept. of Mat'ls Science & Eng.
The Pennsylvania State Univ.
University Park, PA 16802

Prof. D.J. Duquette
Dept. of Metallurgical Eng.
Rensselaer Polytechnic Inst.
Troy, NY 12181

Prof. D. Tomanek
Michigan State University
Dept. of Physics and Astronomy
East Lansing, MI 48824-1116

Dr. M. W. Kendig
Rockwell International Sci.Ctr.
1049 Camino Dos Rios
P.O. Box 1085
Thousand Oaks, CA 91360

Prof. R. A. Rapp
Dept. of Metallurgical Eng.
The Ohio State University
116 West 19th Avenue
Columbus, OH 43210-1179

Dr. R.D. Granata
Zettlemoyer Center for
Surface Studies
Sinclair Laboratory
Lehigh University
Bethlehem, PA 18015

Dr. G. D. Davis
Martin Marietta Laboratories
1450 South Rolling Rd.
Baltimore, MD 21227-3898

Dr. S.M. Lipka
Dept. of Ocean Engineering
Florida Atlantic University
Boca Raton, FL 33431-0991

Prof. J. Kruger
Dept. of Mat'ls Science & Eng.
The Johns Hopkins University
Baltimore, MD 21218

Dr. B.G. Pound
SRI International
333 Ravenswood Ave.
Menlo Park, CA 94025

Prof. C.R. Clayton
Department of Materials Science
& Engineering
State University of New York
Stony Brook
Long Island, NY 11794

Dr. J. W. Oldfield
Cortest Laboratories Ltd
23 Shepherd Street
Sheffield, S3 7BA, England

Ms. D.M. Aylor
Code 2813
David Taylor Research Center
Annapolis, MD 21402-5067

Prof. G. Simkovich
Dept. of Materials Sci. & Eng.
The Pennsylvania State Univ.
University Park, PA 16802

Dr. P.S. Pao
Code 6303
Naval Research Laboratory
Washington, D.C. 20375

Dr. N.S. Bornstein
United Technologies Research Ctr.
East Hartford, CT 06108

Dr. B.A. Shaw
Dept. of Eng. Sci. & Mechanics
228C Hammond Building
The Pennsylvania State University
University Park, PA 16802-1484

Prof. R. M. Latanision
Massachusetts Inst. of Tech.
Room 8-202
Cambridge, MA 02139

Dr. R. E. Ricker
National Institute of Standards and Technology,
Bldg. 223, Room B-266
Gaithersburg, MD 20899

Dr. F.B. Mansfeld
Dept. of Materials Science
University of Southern California
University Park
Los Angeles, CA 900889

Dr. W. R. Bitler
Dept. of Materials Sci. and Eng.
115 Steidle Building
The Pennsylvania State University
University Park, PA 16802

Dr. S. Smialowska
Dept. of Metallurgical Eng.
The Ohio State University
116 West 19th Avenue
Columbus, OH 43210-1179

Dr. R. V. Sara
Union Carbide Corporation
UCAR Carbon Company Inc.
Parma Technical Center
12900 Snow Road
Parma, Ohio 44130

Prof. M.E. Orazem
Dept. of Chemical Engineering
University of Florida
Gainesville, FL 32611

Prof. J. O'M. Bockris
Dept. of Chemistry
Texas A & M University
College Station, TX 77843

Dr. V. S. Agarwala
Code 6062
Naval Air Development Center
Warminster, PA 18974-5000

Prof. Harovel G. Wheat
Dept. of Mechanical Engineering
The University of Texas
ETC 11 5.160
Austin, TX 78712-1063

Prof. S. C. Dexter
College of Marine Studies
University of Delaware
700 Pilottown Rd.
Lewes, DE 19958

Prof. R.P. Gangloff
Dept. of Materials Science & Eng.
Thornton Hall
University of Virginia
Charlottesville, VA 22903-2442

Dr. Wayne C. Tucker
Dept. of Ocean Engineering
University of Rhode Island
Kingston, R.I. 02881

Mr. M. M. Opeka
Code K22
Naval Surface Warfare Center
Silver Spring,MD 20903-5000

Dr. E. McCafferty
Code 6322
Naval Research Laboratory
Washington, D.C. 20375-5000

Dr. R.L. Jones
Naval Research Lab. (Code 6179)
Washington, D.C. 20375-5000